Sparse Shape Model for Fibular Transfer Planning in Mandibular Reconstruction

Riho Kawasaki[1], *Student Member*, *IEEE*, Megumi Nakao[1], *Member*, *IEEE*, Yuichiro Imai[2], Nobuhiro Ueda[3], Toshihide Hatanaka[3], Mao Shiba[3], Tadaaki Kirita[3] and Tetsuya Matsuda[1], *Member*, *IEEE*

***Abstract*— In this paper, we propose an automated preoperative planning method that estimates a plan fitted to the data of a new patient using a planned dataset of previous patients. Although mandibular reconstruction with fibular segments needs preoperative planning for the precise placement of segments, recent interactive planning software cannot secure objectivity of the planning and time-consuming trial-and-error processes are required. The proposed method employs sparse shape modeling; in this modeling, we select a subset of the data from a prepared preoperative planning dataset to make an example or instance of reconstruction via a linear combination of the data. We conduct experiments using the dataset planned by medical doctors and compare the instance estimated by the proposed method to the manual placement by these doctors.**

I. INTRODUCTION

Preoperative planning using computer-aided design with 3D CT data is an active area of research. Appropriate preoperative planning requires standardizing the procedure and securing objectivity. Therefore, the quantification of planning has been studied for surgeries such as mandibular reconstruction [1] and femoral stem implants [2]. However, existing systems require interactive manipulation to determine preoperative planning because appropriate planning varies according to patients. Interactive manipulation causes a lack of objectivity; moreover, this manipulation is time consuming if preoperative planning is complex and has many parameter settings. To solve this problem, the automation of preoperative planning is required.

For mandibular reconstruction using fibula [3], it is necessary to determine osteotomy lines for fibular shaping and the precise placement of fibular segments in the mandible; there are various patterns of fibular placement, as shown in Fig 1. Currently, a trial-and-error process is required for preoperative planning, and surgeons' work and the cost of preoperative planning models are high. A recent study proposed an automatic planning system for mandibular reconstruction [4]; however, the computational cost was high. Therefore, we focus on the use of the past planning data and use a machine learning approach.

In this paper, we propose an automated preoperative planning method for fibular transfer planning in mandibular reconstruction using a dataset of the placement of fibular segments defined in the past. Zhang *et al.* [5] proposed sparse shape composition (SSC) for organ localization and segmentation as a method of shape prior modeling using the accumulated data (training data). This method employs selection of a few datasets that are similar to the input image from a set of the training data based on specific points and approximates an input shape using a weighted linear combination of the data. Sparse linear combination can deal with complex organ shape variations and local details in an input shape. The proposed method introduces sparse shape modeling using SSC to manage the complexities of mandibular shape variations and differences in the resection area. In this framework, we do not use all training datasets but rather a subset whose features are similar to those of the input data to output a proper instance for preoperative planning. This approach can estimate the appropriate fibular placement for each case within a unified framework.

Fig. 1. Examples of fibular transfer planning in the mandible.

We conduct experiments using a dataset planned by medical doctors and compare the plan estimated by the proposed method to the manual placement by these doctors. The results show that our method can predict the appropriate fibular placement with small errors.

II. METHODS

A. Fibular Transfer Planning

We now explain the volumetric fibular transfer planning system [1] used in this study. A user can interactively refine the placement of two or three fibular segments using a patient's CT volume data. The resection area is first determined, then the number of fibular segments is selected (two or three), and finally the position and angle of each segment are refined.

For the fibular transfer planning simulation, we introduce a mathematical description. As shown in Fig 2a, the resection area is determined by the two cutting planes. These are

[1]R. Kawasaki, M. Nakao and T. Matsuda are with Kyoto University, Kyoto, Japan (e-mail: rkawasaki@sys.i.kyoto-u.ac.jp; megumi@i.kyoto-u.ac.jp; tetsu@i.kyoto-u.ac.jp).

[2]Y. Imai is with Rakuwakai Otowa Hospital, Kyoto, Japan (e-mail: rakuwadr1190@rakuwadr.com).

[3]N. Ueda, T. Hatanaka, M. Shiba and T. Kirita are with Nara Medical University, Nara, Japan (e-mail: n-ueda@naramed-u.ac.jp; thatanak@naramed-u.ac.jp; mshiba@naramed-u.ac.jp; tkirita@naramed-u.ac.jp).

978-1-4577-0220-4/16/$31.00 ©2016 IEEE

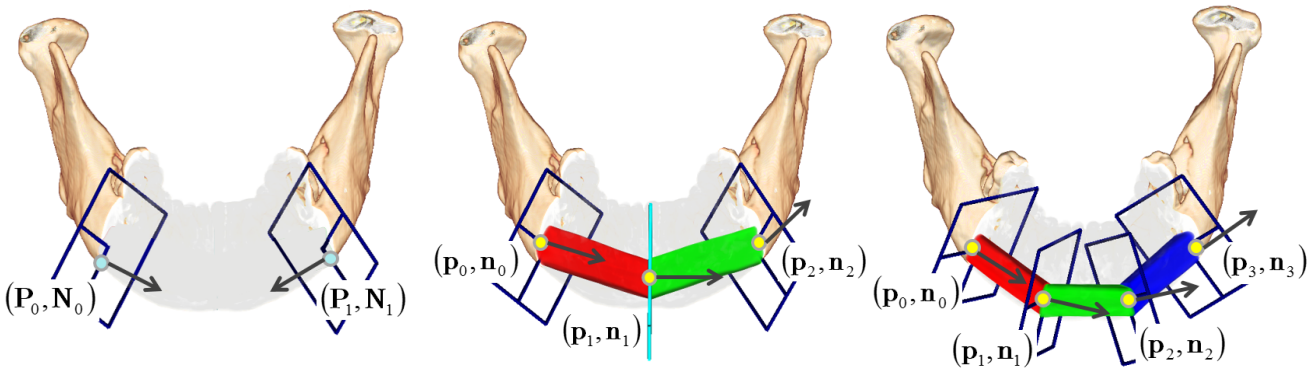

(a) Cutting planes (b) Virtual planes (2-segment) (c) Virtual planes (3-segment)

Fig. 2. Geometrical description of cutting and virtual planes.

defined by a set of 3D vectors $(\mathbf{P}_i, \mathbf{N}_i)$ $(i = 0, 1)$, where $\mathbf{P}_i$ is a point on each cutting plane located at the bottom edge of the mandible and $\mathbf{N}_i$ is the normal vector. The placement of fibular segments is determined by virtual planes, as shown in Figs 2b and 2c. Similar to cutting planes, virtual planes are defined by $(\mathbf{p}_i, \mathbf{n}_i)$ $(i = 0, \cdots, n, n$: the number of fibular segments), where $\mathbf{p}_i$ represents a connection point between a fibular segment and patient's native mandible or another fibular segment. We set $\mathbf{n}_0 = \mathbf{N}_0$ and $\mathbf{n}_n = -\mathbf{N}_1$ because virtual planes $(\mathbf{p}_0, \mathbf{n}_0)$ and $(\mathbf{p}_n, \mathbf{n}_n)$ should equal the corresponding cutting plane. The goal of the proposed method is to approximate the virtual plane $(\mathbf{p}_i, \mathbf{n}_i)$ $(i = 0, \cdots, n)$.

B. Sparse Shape Modeling

In the proposed method, we use the past planning data as the training data, select a subset of the training data that is similar to the input data based on the features of the mandible and resection area, and approximate a suitable placement of fibular segments by a proper combination of the data. To select the appropriate data from the training dataset, we prepare a matrix $\mathbf{D}_f$ containing the information of mandibular features and the resection area of the past preoperative planning data. Then, using the same format data from the input data, we select similar data from the training data via an appropriate minimization problem. The approximation of fibular placement using the selected training data requires the matrix $\mathbf{D}_p$, which includes the information of virtual planes for a reconstruction plan, and the result to be a weighted linear combination of the data. To manage the complexities of mandibular shape variations and differences in the resection area, we hypothesized that a combination of similar training data is better for the approximation than a combination of all datasets, and therefore, we introduce sparse shape modeling.

C. Matrix Representation of Training Data

We introduce the representation of training data matrices $\mathbf{D}_f = [\boldsymbol{d}_f^{(1)} \boldsymbol{d}_f^{(2)} \cdots \boldsymbol{d}_f^{(m)}]$ and $\mathbf{D}_p = [\boldsymbol{d}_p^{(1)} \boldsymbol{d}_p^{(2)} \cdots \boldsymbol{d}_p^{(m)}]$, where column vectors $\boldsymbol{d}_f^{(j)}$ and $\boldsymbol{d}_p^{(j)}$ correspond to the j-th data and m is the number of the training datasets. To form $\mathbf{D}_f$, we define specific points on the mandible. As shown in Fig 3, the five points are landmarks, and each of them is located at the bottom edge of the mandible. The center of the points is the median point of the mandible, and others come in contact with the tangent plane of the bottom edge of the mandible. The normal vectors $\mathbf{N}$ and $\mathbf{n}$ are expressed in Eulerian angles (α, β). To describe the j-th mandible shape, the coordinates of the specific points and points on the cutting plane $\mathbf{P}_i$ $(i = 0, 1)$ and (α, β) corresponding to $\mathbf{N}_i$ $(i = 0, 1)$ are arranged into the column vector $\boldsymbol{d}_f^{(j)}$. Therefore, $\boldsymbol{d}_f^{(j)}$ has 25 dimensions. Next, we transfer the information of virtual planes into the training data $\mathbf{D}_p$. To make the two virtual planes, i.e., $(\mathbf{p}_0, \mathbf{n}_0)$ and $(\mathbf{p}_n, \mathbf{n}_n)$, equal to the corresponding cutting plane, connection points between a fibular segment and mandible need to be located on this plane. Therefore, an $x'y'$ orthogonal coordinate system is identically defined on each cutting plane, and the coordinate of each connection point is represented as $a\boldsymbol{e}_{x'} + b\boldsymbol{e}_{y'}$, where $\boldsymbol{e}_{x'}$ or $\boldsymbol{e}_{y'}$ is a unit vector in the direction of the x' or y' axis, respectively. Then, the coordinates of the connection points $\mathbf{p}_i$ $(i = 1, \cdots, n-1)$, (a, b) corresponding to $\mathbf{p}_i$ $(i = 0, n)$ and (α, β) corresponding to $\mathbf{n}_i$ $(i = 1, \cdots, n-1)$ are arranged into the column vector $\boldsymbol{d}_p^{(j)}$. Accordingly, $\boldsymbol{d}_p^{(j)}$ will be 9-dimensional or 14-dimensional for 2-segment or 3-segment, respectively. In our framework, all training datasets are pre-aligned using a generalized Procrustes analysis [6] based on the five specific points. Specifically, all points are translated so that the mean of the five points is translated to the origin, scaled so that the root-mean-square distance from the translated origin is 1, rotated so that the median point of the mandible is on the y axis about the origin, and rotated so that the mandible is parallel to the $x - y$ plane about the y axis.

D. Objective Function

Using the training data matrices $\mathbf{D}_f$ and $\mathbf{D}_p$, we approximate virtual planes fitted to the input data via a minimization problem. First, we extract the information of mandibular features and the resection area from the input data to make a vector $\boldsymbol{y}$ by following the same procedure of $\boldsymbol{d}_f^{(i)}$. To

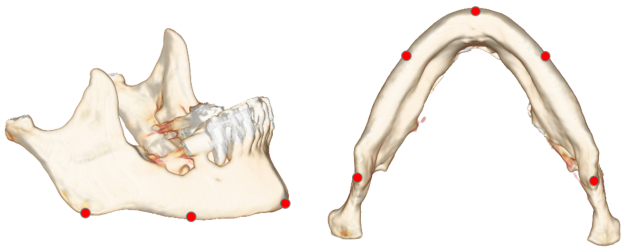

Fig. 3. Definition of feature points on the mandible.

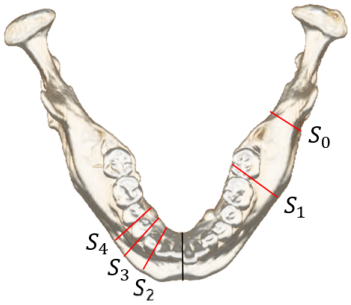

Fig. 4. Five cutting planes based on anatomical features of the mandible.

approximately represent the input $\boldsymbol{y}$ by a weighted sparse linear combination, denoting $\hat{\boldsymbol{x}} = [x_1, x_2, \cdots, x_m]^T \in \mathbb{R}^m$ as the weights, we calculate the weights by solving

$$\hat{\boldsymbol{x}} = \arg\min_{\boldsymbol{x}} ||\boldsymbol{y} - \mathbf{D}_f \boldsymbol{x}||_2^2 \quad \text{such that :} \quad ||\boldsymbol{x}||_0 \leq k, \tag{1}$$

where $||\cdot||_0$ is the $L0$ norm and k is the sparsity number. However, Eq. (1) is not directly tractable because of the computational complexity caused by the non-convexity of the $L0$ norm. Therefore, we introduce recent developments to solve this type of problems via $L1$ norm relaxation, and our objective function is represented by

$$\hat{\boldsymbol{x}} = \arg\min_{\boldsymbol{x}} ||\boldsymbol{y} - \mathbf{D}_f \boldsymbol{x}||_2^2 + \lambda ||\boldsymbol{x}||_1, \tag{2}$$

where λ is a parameter to control the sparsity. This problem is efficiently solved using an alternating minimization framework. Then, $\mathbf{D}_p \hat{\boldsymbol{x}}$ is calculated as the placement of virtual planes for the input data and transformed back using the corresponding inverse matrix of normalization.

III. EXPERIMENTS

The performance of the proposed method has been evaluated via experiments using a dataset planned by surgeons, and the gap between the manual placement by the surgeons was then calculated.

A. Experimental Setting

Ten CT datasets obtained from both the head and foot were applied to the developed software. The CT slice images were first re-sampled as regularized volume data with 256^3 voxels. The mandible region was extracted from the head CT data, and the fibular image was extracted from the foot CT data. Then, the five feature points defined in section II-C were manually determined and normalized using Procrustes analysis. To observe the differences in the resection areas, we defined six types of resection areas for each dataset. As shown in Fig 4, five cutting planes S_i $(i = 0, \cdots, 4)$ were defined based on anatomical distinctions, specifically S_0: mandibular ramus, S_1: midpoint of chin and S_0, S_2: midpoint of chin and S_4, S_3: midpoint of S_2 and S_4, and S_4: mental foramen. The resection areas were represented as $S_0 - S_2$, $S_0 - S_3$, $S_0 - S_4$, $S_1 - S_2$, $S_1 - S_3$ and $S_1 - S_4$. The appropriate fibular placements with 2-segment were given by surgeons in these sixty instances.

We performed 10-fold cross-validation, i.e., we used one case (six instances) for the input data and the others (fifty-four instances) for the training data. To estimate the virtual planes, the training data matrices $\mathbf{D}_f$ and $\mathbf{D}_p$, and the input vector $\boldsymbol{y}$ were described from the fifty-four training data and the input instance, respectively. Then, we calculated the weighting vector $\hat{\boldsymbol{x}}$ by solving Eq. (2) using the Fast Iterative Shrinkage-Thresholding Algorithm (FISTA) [7] and estimated the proper virtual planes given by $\mathbf{D}_p \hat{\boldsymbol{x}}$. In Eq. (2), we chose $\lambda = 0.05$ based on some estimation results. For comparison, we also considered the case where the idea of sparsity was not introduced ($\lambda = 0$ in Eq. (2)) and only the best-fit training data were used. The best-fit data were selected by $\min_j ||\boldsymbol{y} - \boldsymbol{d}_f^{(j)}||_2^2$. To compare the error between the estimation results and the manual placement of the surgeons, we introduced a distance error and an angle error. The distance error was calculated from the mean distance of the three connection points, and the angle error was defined by the angle formed by the normal vector of the virtual planes not fitted to the cutting planes.

B. Automated Planning Results

The results for Case 1 with resection area $S_0 - S_2$ and $S_1 - S_3$ are shown in Fig 5. In the former case ($S_0 - S_2$), all methods achieved virtual planes with similar positions and directions to the surgeons' definition. However, in the latter case ($S_1 - S_3$), the proposed method clearly shows the best performance. The middle virtual plane was located close to the chin and the angle was approximately the same as the manual placement. To compare the results quantitatively, we evaluated the distance error and the angle error between the approximate results and the manual placement by the surgeons for the sixty instances. In Fig 6, the x-mark is the mean value, the center-line is the median, the edges of the box are the 25th and 75th percentiles and the whiskers extend to the most extreme data points. Both errors for the proposed method were the smallest of the various methods tested, and the variances were also small.

IV. CONCLUSIONS

This paper proposed sparse shape modeling for automated fibular transfer planning in mandibular reconstruction. Sparse

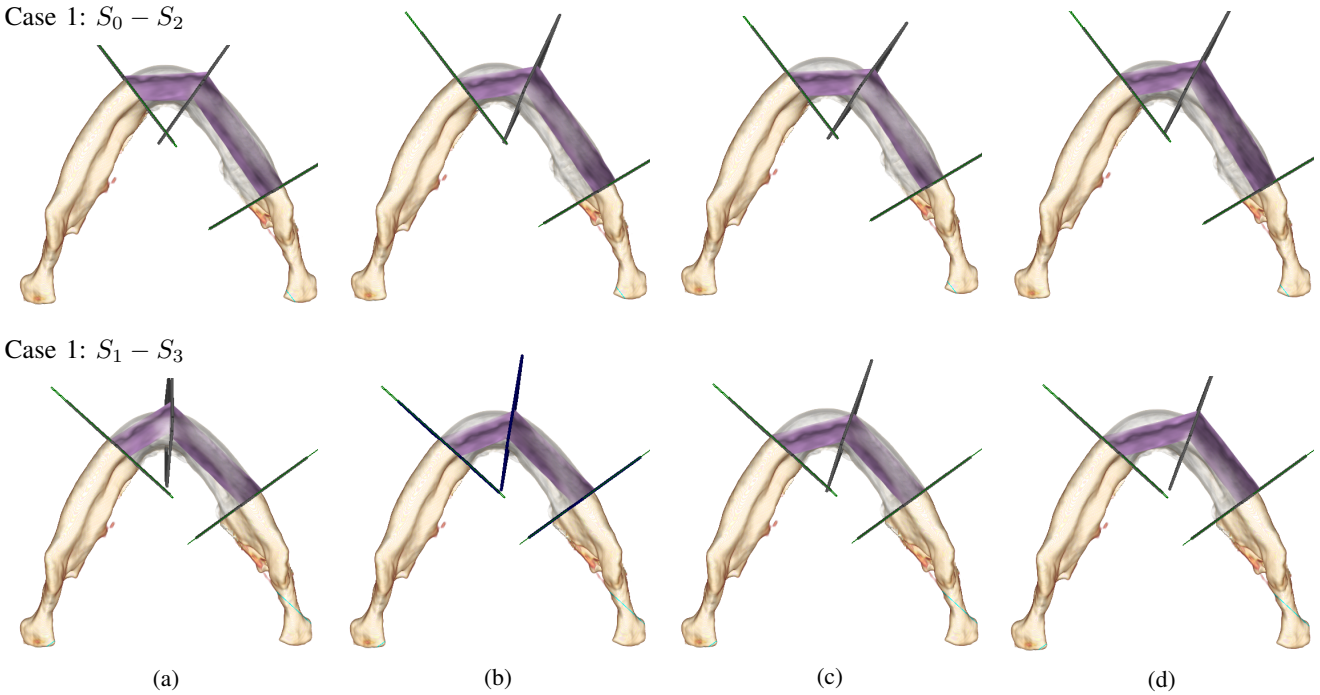

Fig. 5. Comparison of fibular transfer planning results for (a) the manual placement given by surgeons, (b) the proposed sparse modeling ($\lambda = 0.05$), (c) the non-sparse modeling ($\lambda = 0$), and (d) the best-fit training data.

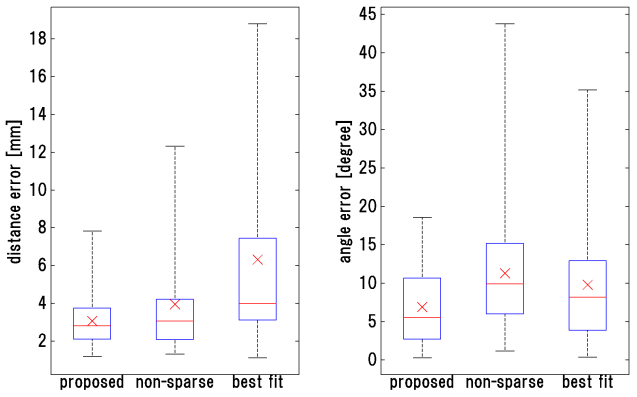

Fig. 6. Estimation errors of the three methods.

linear combination of the training data achieved proper fibular placement for the input data. The experiments using a dataset planned by surgeons showed results similar to the surgeons' definition. Our proposed method outperformed the other methods in a comparison of the estimation error. The results verified the effectiveness of sparse shape modeling.

ACKNOWLEDGMENTS

This research was supported by JSPS Grant-in-Aid for Scientific Research (B) (15H03032) and the Center of Innovation (COI) Program of the Japan Science and Technology Agency (JST).

REFERENCES

[1] M. Nakao, M. Hosokawa, Y. Imai, N. Ueda, T. Hatanaka, T. Kirita and T. Matsuda, "Volumetric Fibular Transfer Planning With Shape-Based Indicators in Mandibular Reconstruction," *IEEE Journal of Biomedical and Informatics*, Vol. 19, No. 2, pp. 581-589, 2015.

[2] I. Otomaru, M. Nakamoto, Y. Kagiyama, M. Takao, N. Sugano, N. Tomiyama, Y. Tada and Y. Sato, "Automated preoperative planning of femoral stem in total hip arthroplasty from 3D data: Atlas-based approach and comparative study," *Medical Image Analysis*, Vol. 16, No. 2, pp. 415-426, 2012.

[3] A. F. Flemming, M. D. Brough, N. D. Evans, H. R. Grant, M. Harris, D. R. James, M. Lawlor and I. M. Laws, "Mandibular reconstruction using vascularised fibula," *Brit. J. Plastic Surg.*, Vol. 43, No. 4, pp. 403-409, 1990.

[4] S. Aso, M. Nakao, K. Imanishi, Y. Imai, N. Ueda, T. Hatanaka, T. Kirita and T. Matsuda, "A Study on Semi-automatic Fibular Transfer Planning in Mandibular Reconstruction," in *Proc. Medical and Biological Imaging*, pp. 6, 2015.

[5] S. Zhang, Y. Zhan, M. Dewan, J. Huang, D. N. Metaxas, and X. S. Zhou, "Towards robust and effective shape modeling: Sparse Shape Composition," *Medical Image Analysis*, Vol. 16, No. 1, pp. 265-277, 2012.

[6] C. Gooball, "Procrustes Methods in the Statistical Analysis of Shape," *Journal of the Royal Statistical Society*, Vol. 53, No. 2, pp. 285-339, 1991.

[7] A. Beck and M. Teboulle, "A fast iterative shrinkage-thresholding algorithm for linear inverse problems," SIAM J. Imaging Science, Vol.2, pp. 183-202, 2009.